

Supporting Information

Architecting NiFe-LDH/MXene nano-arrays hybrid toward exceptional capacitive lithium storage

Jian Shen, Guangxu Yang, Guangbin Duan*, Xi Guo, Li Li*, Bingqiang

Cao

School of Materials Science and Engineering, University of Jinan, Jinan
250022, Shandong, China

*Corresponding authors at: School of Materials Science and Engineering,
University of Jinan, Jinan 250022, PR China.

Tel.: +86 531 82765473; fax: +86 531 87974453.

E-mail addresses: mse_lil@ujn.edu.cn (L. Li), mse_duangb@ujn.edu.cn

(G. Duan)

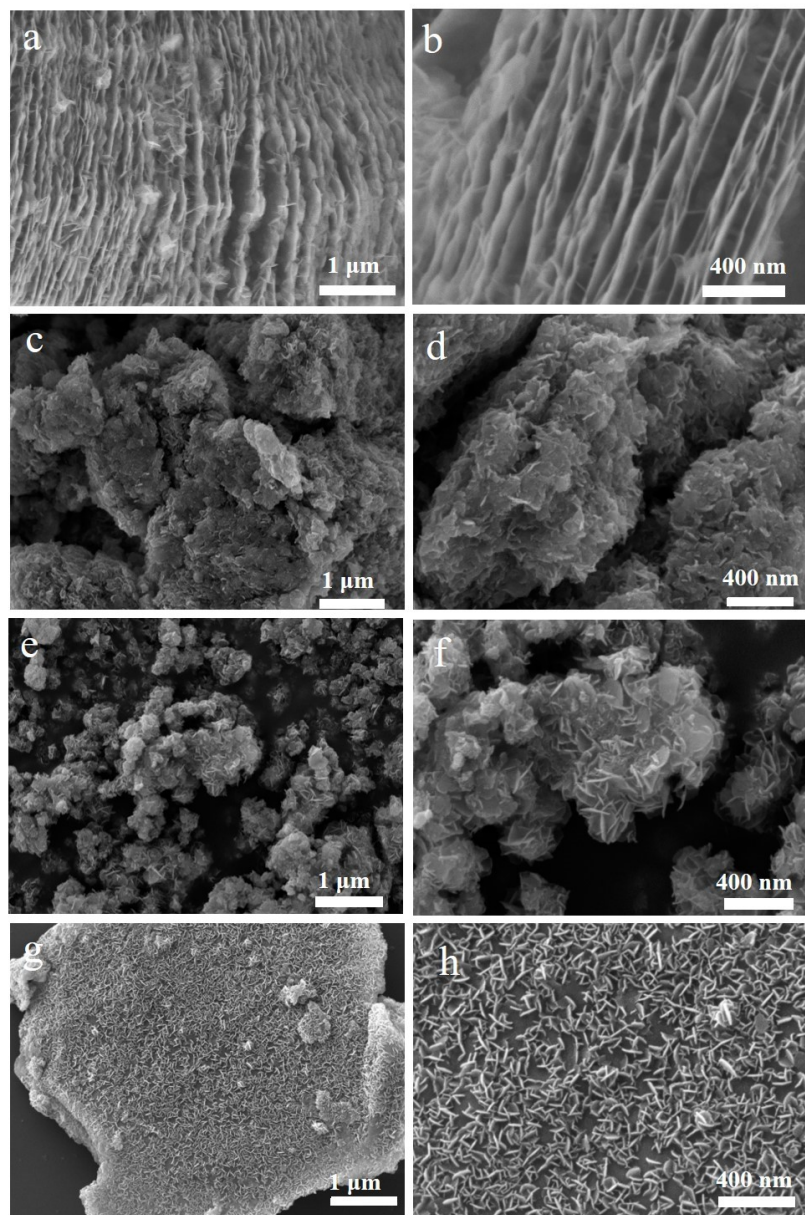


Figure S1. SEM images of (a-b) Ti₃C₂T_x-MXene, (c-d) NiFe-LDH, (e-f) NiFe-LDH /MXene-50, (g-h) NiFe-LDH /MXene-200.

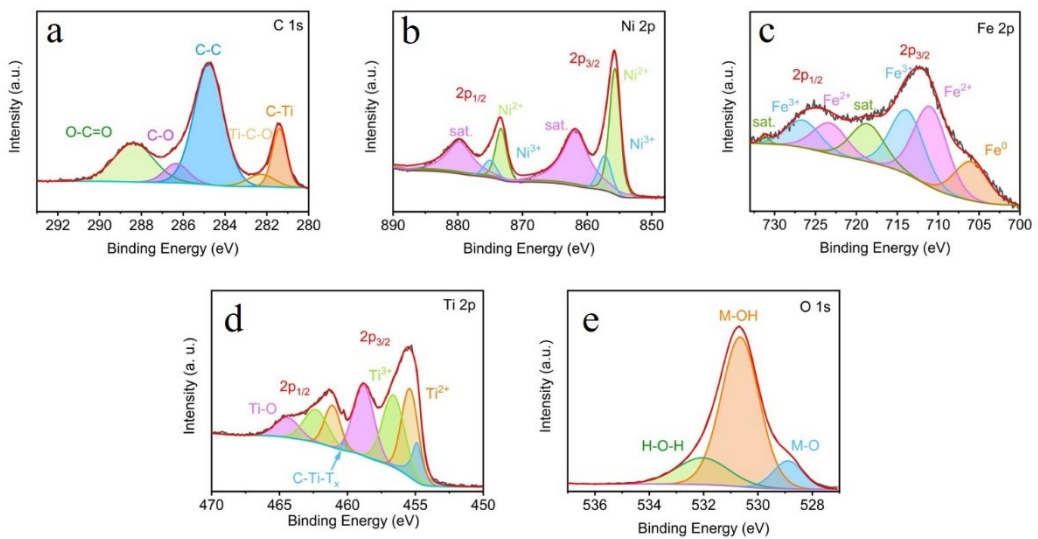


Figure S2. High-resolution XPS spectra of (a) C 1s, (b) Ni 2p, (c) Fe 2p, (d) Ti 2p, (e) O 1s for NiFe-LDH/MXene-500.

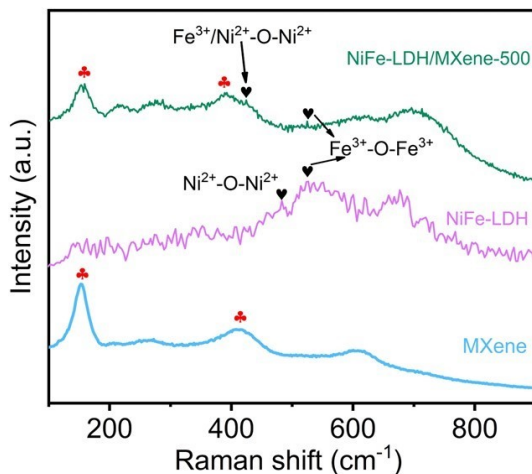


Figure S3. Raman spectra of NiFe-LDH, Mxene and NiFe-LDH /MXene-500.

Table S1. The specific surface areas and total pore volumes of the samples.

| Electrode | NiFe-LDH | NiFe-LDH/MXene-50 | NiFe-LDH/MXene-200 | NiFe-LDH/MXene-500 | MXene |
|---|----------|-------------------|--------------------|--------------------|--------|
| materials | LDH | LDH/MXene | LDH/MXene | LDH/MXene | |
| | | -50 | -200 | -500 | |
| Specific surface area ($\text{m}^2 \text{ g}^{-1}$) | 223.3 | 77.77 | 54.98 | 41.07 | 2.04 |
| Total pore volume ($\text{cm}^3 \text{ g}^{-1}$) | 0.439 | 0.2908 | 0.1691 | 0.1305 | 0.0181 |
| | | 1 | 9 | | |

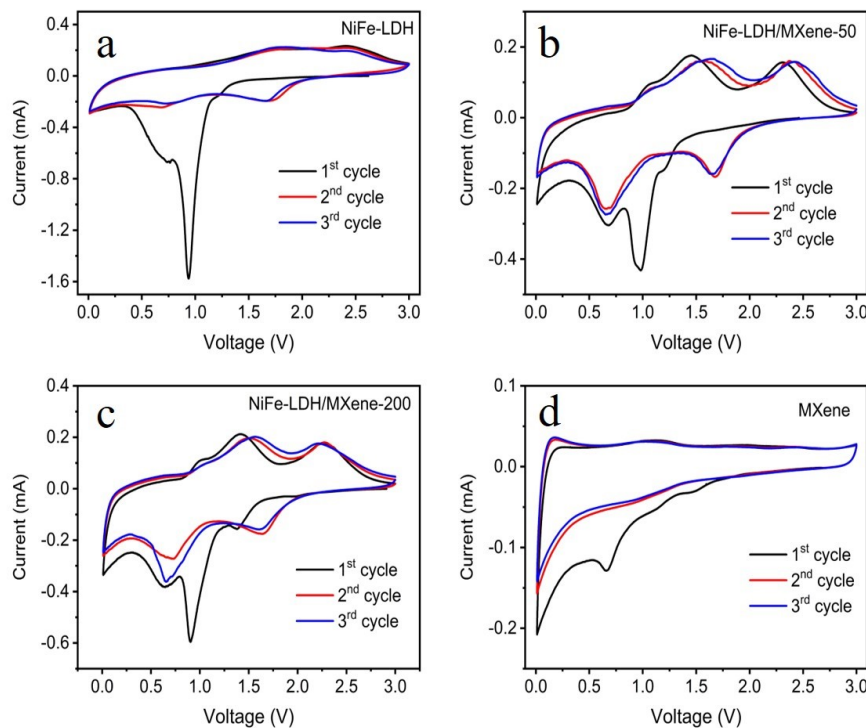


Figure S4. CV curves at a scan rate of 0.2 mV s^{-1} for (a) NiFe-LDH, (b)NiFe-LDH/MXene-50, (c) NiFe-LDH/MXene-200 and (d) MXene.

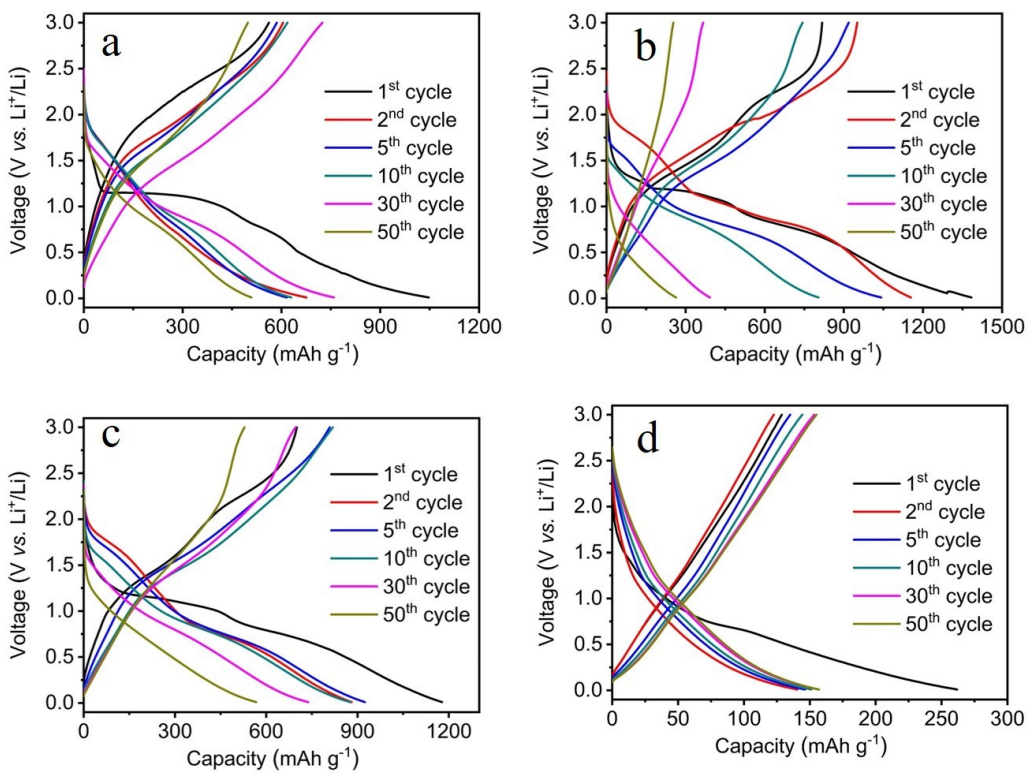


Figure S5. GCD profiles of (a)NiFe-LDH, (b) NiFe-LDH/MXene-50, (c) NiFe-LDH/Mxene-200, (d) MXene.

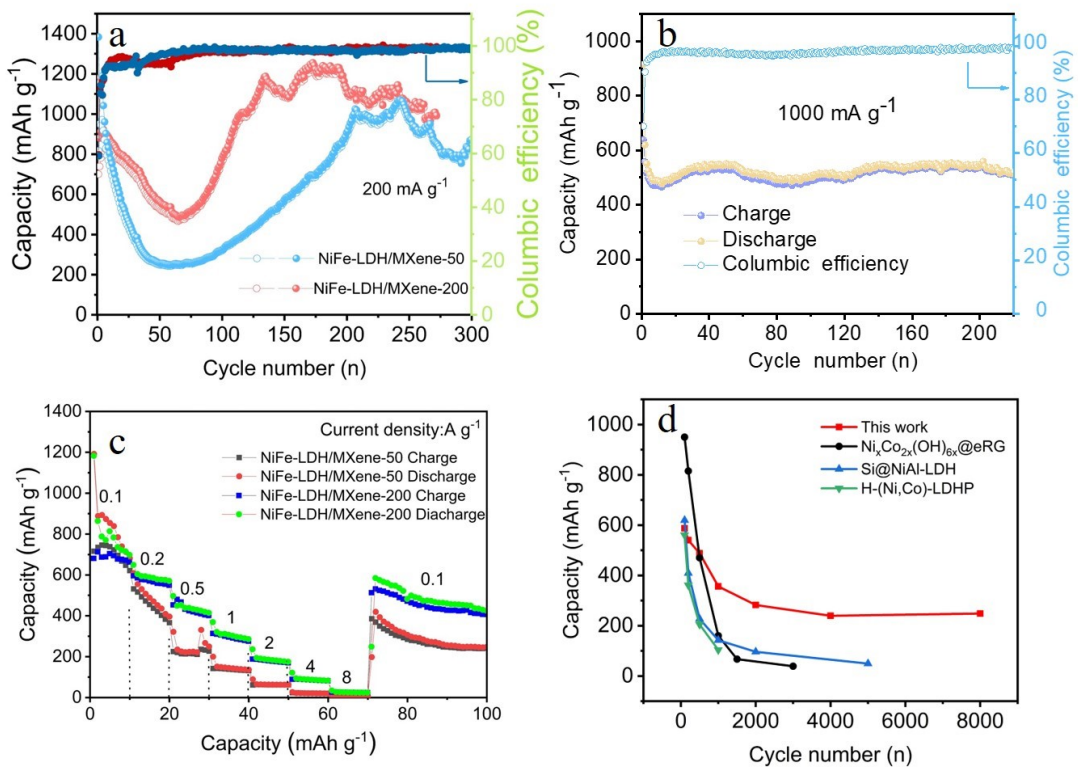


Figure S6. (a) Comparison of cyclability of the NiFe-LDH and MXene at 200 mA g⁻¹. (b) Cycling performance of the NiFe-LDH/MXene-500 electrode at 1000 mA g⁻¹. (c) Comparison of rate capacity of the NiFe-LDH/MXene hybrid materials. (d) Comparisons in the rate capabilities between this work and other LDH-based electrodes.

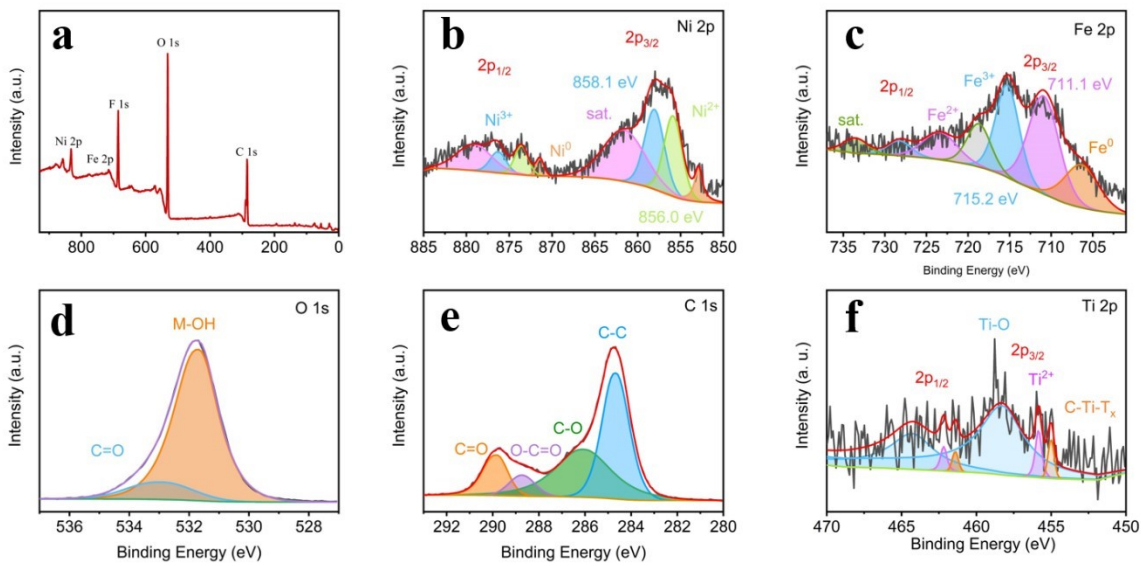


Figure S7. XPS spectra of (a) survey scan; (b-c) Fe 2p, and Ni 2p of NiFe-LDH/MXene

hybrid materials and NiFe-LDH; and (d) Ti 2p of NiFe-LDH/MXene-500 electrodes after 50 cycles.

Table S2. Comparison of electrochemical performance of LDH-based materials in LIBs.

| Materials | Cycling performance (mAh g ⁻¹ at A g ⁻¹) | Rate performance (mAh g ⁻¹ at A g ⁻¹) | Ref. |
|--|---|--|------|
| Ni _x Co _{2x} (OH) _{6x} @eRG | 373.0 at 1 (500 cycles) | 950.0 at 0.1, 160.0 at 1 | 1 |
| Si@NiAl-LDH | 534.0 at 0.05 (60 cycles) | 619.5 at 0.1, 142.3 at 1 | 2 |
| H-(Ni,Co)-LDHP | 355.4 at 0.1 (50 cycles) | 560.3 at 0.1, 103.6 at 1 | 3 |

Reference

- [1] J. Shi, N. Du, W. Zheng, X. Li, Y. Dai, G. He, Ultrathin Ni-Co double hydroxide nanosheets with conformal graphene coating for highly active oxygen evolution reaction and lithium ion battery anode materials, *Chem. Eng. J.*, 327 (2017) 9-17.
- [2] Q. Li, Y. Wang, B. Lu, J. Yu, M. Yuan, Q. Tan, Z. Zhong, F. Su, Hollow core-shell structured Si@NiAl-LDH composite as high-performance anode material in lithium-ion batteries, *Electrochim. Acta*, 331 (2020) 135331.
- [3] Y. Lu, Y. Du, H. Li, Template-sacrificing synthesis of Ni-Co layered double hydroxides polyhedron as advanced anode for lithium ions battery, *Front. Chem.*, 8 (2020) 581653.